

A simple locking-free discrete shear triangular plate element

Y.C. Cai^{1,2,3}, L.G. Tian¹ and S.N. Atluri³

Abstract: A new three node triangular plate element, labeled here as DST-S6 (Discrete Shear Triangular element with 6 extra Shear degrees of freedom), is proposed for the analyses of plate/shell structures comprising of thin or thick members. The formulation is based on the DKT (Discrete Kirchhoff Technique) and an appropriate use of the independent shear DOF(Degrees Of Freedom). The shear locking is completely eliminated in the DST-S6, without any numerical expedencies such as the reduce integration, the use of assumed strains/stresses, or the need for the stabilization of the attendant zero energy modes. It is shown that the present DST-S6 is much simpler than the triangular shear-deformable plate elements currently available which pass the patch test for thick to very thin plates. The DST-S6 has two extra shear DOF per node, but the extra shear DOF are the rotations caused by the transverse shear deformation, and there is no difficulty in applying the essential boundary conditions for the present DST-S6. It is also demonstrated that the solution of a pressure-loaded simply-supported circular plate of the DST-S6 avoids the so-called polygon-circle Paradox. Various numerical examples indicate that the DST-S6 is a robust and high-performance element for thick and thin plates.

Keywords: plate/shell element, locking-free, discrete Kirchhoff theory, triangular element, shear degrees of freedom

1 Introduction

Plate/Shell structures play an important role in civil, naval and airspace engineering. There has been a great interest in high performance coupled with simple formulation, in the field of finite elements for plates and shells over the past several decades (Gal and Levy 2006; Cai, Paik and Atluri 2010; Iura and Atluri 2003).

¹ Key Laboratory of Geotechnical and Underground Engineering of Ministry of Education, Department of Geotechnical Engineering, Tongji University, Shanghai 200092, P.R.China

² Corresponding author. Email: yc_cai@163.net.

³ Center for Aerospace Research & Education, University of California, Irvine

The existing Mindlin plate elements can be broadly divided into two main groups. The first group is the displacement model based on the assumed displacement function of the element, while the second group uses the mixed/hybrid element method. The Mindlin-Reissner plate theory for the analyses of thin and thick plates requires only a C^0 continuity for the transverse displacement as well as the normal rotations, and the difficulties of C^1 continuity requirement for the transverse displacement for the Kirchhoff elements can be avoided. However, the Mindlin-Reissner plate elements based on the displacement approach give poor results in thin plate limit because of the shear locking phenomenon. In order to eliminate the shear locking in the Mindlin-Reissner plate elements, reduced integration, assumed natural strain (ANS) approach, and assumed stress elements (or mixed/hybrid stress elements) are used. For example, the reduced integration method by Zienkiewicz, Taylor and Too(1971), and Pugh, Hinton and Zienkiewicz (1978), the selective integration method by Malkus and Hughes(1978), and Hughes Cohen and Haroun (1978), the MITC family by Bathe and Dvorkin (1985), the MISC element by Nguyen, Rabczuk, Stephane and Debongnie (2008), the DST family by Batoz and Lardeur (1992), and Batoz and Katili (1992), the RDKTM by Chen and Cheung (2001), the hybrid-Trefftz plate elements by Choo, Choi and Lee (2010), the assumed stress/strain elements by Lee and Pian (1978), Katili(1993), and Brasile (2008). Most of these elements are free from shear locking and are very useful for practical applications. However, these popular elements always involve very complex formulations to take the transverse shear effects into account for thick plates, and thus lead to complexity in the form, and difficulty in the programming, of the stiffness matrix.

In this work, we present a simple three node triangular plate element, labeled here as DST-S6 (Discrete Shear Triangular element with 6 extra Shear degrees of freedom), for the analyses of plate/shell structures comprising of thin or thick members. The formulation is based on the DKT (Discrete Kirchhoff Technique) (Batoz, Bathe and Ho 1980; Dhatt 1969) and an appropriate use of the independent shear DOF (Atluri 2005; Li, Soric, Jarak and Atluri 2005). The shear locking is completely eliminated in the DST-S6, without any numerical expediences such as the reduced integration, the use of assumed strains/stresses, or the need for the stabilization of the attendant zero energy mode. It is shown that the present DST-S6 is much simpler than the triangular shear-deformable plate elements currently available, which also pass the patch test for thick to very thin plates.

2 Interpolation functions

2.1 The DKT element in brief

Consider a linear elastic triangular plate element undergoing infinitesimal deformation, as shown in Fig.1. The derivatives of the transverse displacement w around two independent axes (not including the influence of the transverse shear deformation) are

$$\tilde{\theta}_x = \frac{\partial w}{\partial x}, \tilde{\theta}_y = \frac{\partial w}{\partial y} \tag{1}$$

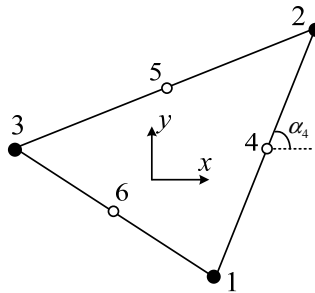


Figure 1: Triangular element

The constraints of the zero-transverse-shear Kirchhoff plate theory are presented in the following discrete way:

at the corner nodes i ($i = 1, 2, 3$)

$$\tilde{\theta}_{xi} = \frac{\partial w}{\partial x} \Big|_{\mathbf{x}=\mathbf{x}_i}, \tilde{\theta}_{yi} = \frac{\partial w}{\partial y} \Big|_{\mathbf{x}=\mathbf{x}_i} \tag{2}$$

at the mid-side points k ($k = 4, 5, 6$)

$$\tilde{\theta}_{nk} = \frac{1}{2} (\tilde{\theta}_{ni} + \tilde{\theta}_{nj}) \tag{3}$$

$$\tilde{\theta}_{sk} = \frac{\partial w}{\partial s} \Big|_{\mathbf{x}=\mathbf{x}_k} = \frac{1.5}{l_k} (w_j - w_i) - \frac{1}{4} (\tilde{\theta}_{si} + \tilde{\theta}_{sj}) \tag{4}$$

where $\mathbf{x}_i = (x_i, y_i)$ are the coordinates of the node i ; s and n indicate the tangent and normal of the element side ij respectively; l_k is the length of side ij ; $i = 1, 2, 3$ and $j = 2, 3, 1$ when $k = 4, 5, 6$.

Along each side ij we have

$$\begin{Bmatrix} \tilde{\theta}_{sk} \\ \tilde{\theta}_{nk} \end{Bmatrix} = \begin{bmatrix} m_k & n_k \\ -n_k & m_k \end{bmatrix} \begin{Bmatrix} \tilde{\theta}_{xk} \\ \tilde{\theta}_{yk} \end{Bmatrix} \tag{5}$$

where $m_k = \cos \alpha_k$ and $n_k = \sin \alpha_k$ when $k = 4, 5, 6$.

The rotations $\tilde{\theta}_x$ and $\tilde{\theta}_y$ of the element can be defined as follows:

$$\tilde{\theta}_x = \sum_{i=1}^6 N_i \tilde{\theta}_{xi}, \quad \tilde{\theta}_y = \sum_{i=1}^6 N_i \tilde{\theta}_{yi} \tag{6}$$

where

$$\begin{aligned} N_j &= (2L_j - 1)L_j \quad (j = 1, 2, 3) \\ N_4 &= 4L_1L_2, N_5 = 4L_2L_3, N_6 = 4L_3L_1 \end{aligned} \tag{7}$$

L_i are the area coordinates of the three-node triangular plate element and can be expressed as

$$L_i = \frac{1}{2A} (a_i + b_i x + c_i y) \tag{8}$$

$$a_i = x_j y_m - x_m y_j, \quad b_i = y_j - y_m, \quad c_i = -x_j + x_m \tag{9}$$

where A is the area of the triangular element, and $i = 1, 2, 3; j = 2, 3, 1; m = 3, 1, 2$.

Finally, the following DKT displacements in each plate element are obtained by using Eqs.(2) to (6):

$$\begin{aligned} \tilde{\theta}_x &= \sum_{i=1}^3 (R_i w_i + R_{xi} \tilde{\theta}_{xi} + R_{yi} \tilde{\theta}_{yi}) \\ \tilde{\theta}_y &= \sum_{i=1}^3 (H_i w_i + H_{xi} \tilde{\theta}_{xi} + H_{yi} \tilde{\theta}_{yi}) \end{aligned} \tag{10}$$

where

$$R_1 = 1.5 (m_6 N_6 / l_6 - m_4 N_4 / l_4), \quad R_2 = 1.5 (m_4 N_4 / l_4 - m_5 N_5 / l_5),$$

$$R_3 = 1.5 (m_5 N_5 / l_5 - m_6 N_6 / l_6),$$

$$R_{x1} = N_1 + N_4 (0.5n_4^2 - 0.25m_4^2) + N_6 (0.5n_6^2 - 0.25m_6^2),$$

$$R_{x2} = N_2 + N_4 (0.5n_4^2 - 0.25m_4^2) + N_5 (0.5n_5^2 - 0.25m_5^2),$$

$$\begin{aligned}
 R_{x3} &= N_3 + N_5 (0.5n_5^2 - 0.25m_5^2) + N_6 (0.5n_6^2 - 0.25m_6^2), \\
 R_{y1} &= -0.75 (m_4n_4N_4 + m_6n_6N_6), \\
 R_{y2} &= -0.75 (m_4n_4N_4 + m_5n_5N_5), \\
 R_{y3} &= -0.75 (m_5n_5N_5 + m_6n_6N_6); \\
 H_1 &= 1.5 (n_6N_6/l_6 - n_4N_4/l_4), \quad H_2 = 1.5 (n_4N_4/l_4 - n_5N_5/l_5), \\
 H_3 &= 1.5 (n_5N_5/l_5 - n_6N_6/l_6), \quad H_{x1} = R_{y1}, \quad H_{x2} = R_{y2}, \quad H_{x3} = R_{y3}, \\
 H_{y1} &= N_1 + N_4 (0.5m_4^2 - 0.25n_4^2) + N_6 (0.5m_6^2 - 0.25n_6^2), \\
 H_{y2} &= N_2 + N_4 (0.5m_4^2 - 0.25n_4^2) + N_5 (0.5m_5^2 - 0.25n_5^2), \\
 H_{y3} &= N_3 + N_5 (0.5m_5^2 - 0.25n_5^2) + N_6 (0.5m_6^2 - 0.25n_6^2)
 \end{aligned}$$

2.2 The displacement functions of the proposed element DST-S6

For the three node element DST-S6 as shown in Fig.2, the shear strains are assumed as

$$\gamma_x = \sum_{i=1}^3 (L_i \gamma_{xi}), \gamma_y = \sum_{i=1}^3 (L_i \gamma_{yi}) \tag{11}$$

where γ_{xi} and γ_{yi} are the independent shear DOF of node i .

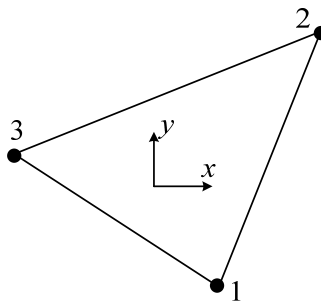


Figure 2: Three-node triangular plate element

The total rotations θ_x and θ_y of the thick plate (including the influence of the transverse shear deformation) can be given by

$$\theta_x = \tilde{\theta}_x - \gamma_x, \theta_y = \tilde{\theta}_y - \gamma_y \tag{12}$$

Substituting Eqs.(10) and (11) into Eq.(12), and noticing that $\tilde{\theta}_{xi} = \theta_{xi} + \gamma_{xi}$ and $\tilde{\theta}_{yi} = \theta_{yi} + \gamma_{yi}$ at node i , one obtains

$$\begin{aligned} \theta_x &= \sum_{i=1}^3 [R_i w_i + R_{xi} \theta_{xi} + R_{yi} \theta_{yi} + (R_{xi} - L_i) \gamma_{xi} + R_{yi} \gamma_{yi}] \\ \theta_y &= \sum_{i=1}^3 [H_i w_i + H_{xi} \theta_{xi} + H_{yi} \theta_{yi} + H_{xi} \gamma_{xi} + (H_{yi} - L_i) \gamma_{yi}] \end{aligned} \tag{13}$$

Thus, the matrix form of the generalized displacement functions of the DST-S6 can be expressed as

$$\mathbf{U} = \Phi \mathbf{a} = \begin{bmatrix} \Phi_1 & \Phi_2 & \Phi_3 \end{bmatrix} \begin{Bmatrix} \mathbf{a}_1 \\ \mathbf{a}_2 \\ \mathbf{a}_3 \end{Bmatrix} \tag{14}$$

where

$$\mathbf{U} = [\theta_x \quad \theta_y \quad \gamma_x \quad \gamma_y]^T \tag{15}$$

$$\mathbf{a}^i = [w_i \quad \theta_{xi} \quad \theta_{yi} \quad \gamma_{xi} \quad \gamma_{yi}]^T \tag{16}$$

$$\Phi_i = \begin{bmatrix} R_i & R_{xi} & R_{yi} & R_{xi} - L_i & R_{yi} \\ H_i & H_{xi} & H_{yi} & H_{xi} & H_{yi} - L_i \\ 0 & 0 & 0 & L_i & 0 \\ 0 & 0 & 0 & 0 & L_i \end{bmatrix} \tag{17}$$

Notice that γ_{xi} and γ_{yi} in Eq.(16) are retained as independent shear DOF of node i , which lead to a locking-free element which remains uniformly valid for either thick or thin plates/shells, without using such numerical expediciencies as selective/reduced integrations and without the need for stabilizing the attendant spurious modes of zero-energy.

3 Stiffness matrix of the DST-S6

For deriving the element stiffness matrix of DST-S6 element, the strain energy in an element can be written as (Chen and Cheung 2001)

$$\Pi_p = \frac{1}{2} \int_{A_e} (\boldsymbol{\chi}^T \mathbf{D}_b \boldsymbol{\chi} + \boldsymbol{\gamma}^T \mathbf{D}_s \boldsymbol{\gamma}) dx dy \tag{18}$$

in which $\boldsymbol{\chi}$ is the bending stain, $\boldsymbol{\gamma}$ is the shear strain

$$\boldsymbol{\chi} = \left[\frac{\partial \theta_x}{\partial x}, \quad \frac{\partial \theta_x}{\partial y}, \quad \frac{\partial \theta_x}{\partial y} + \frac{\partial \theta_y}{\partial x} \right]^T, \boldsymbol{\gamma} = [\gamma_x \quad \gamma_y]^T \tag{19}$$

and

$$\mathbf{D}_b = \frac{Eh^3}{12(1-\nu^2)} \begin{bmatrix} 1 & \nu & 0 \\ \nu & 1 & 0 \\ 0 & 0 & \frac{1-\nu}{2} \end{bmatrix}, \mathbf{D}_s = \frac{5Eh}{12(1+\nu)} \begin{bmatrix} 1 & 0 \\ 0 & 1 \end{bmatrix} \quad (20)$$

where E is the elastic modulus, ν is the Poisson ratio, and h is the thickness of the plate element.

Substituting Eq.(14) into Eq.(18), the element stiffness matrix of the DST-S6 can be written as

$$\mathbf{K}^e = \mathbf{K}_b^e + \mathbf{K}_s^e \quad (21)$$

in which the bending part and the shear transverse-strain part of the element stiffness matrix can be respectively written as

$$\mathbf{K}_b^e = \int_{A_e} \mathbf{B}_b^T \mathbf{D}_b \mathbf{B}_b dx dy, \mathbf{K}_s^e = \int_{A_e} \mathbf{B}_s^T \mathbf{D}_s \mathbf{B}_s dx dy \quad (22)$$

where

$$\mathbf{B}_b = [\mathbf{B}_{b1} \quad \mathbf{B}_{b2} \quad \mathbf{B}_{b3}] \quad (23)$$

$$\mathbf{B}_{bi} = \begin{bmatrix} R_{i,x} & R_{xi,x} & R_{yi,x} & R_{\gamma i,x} & R_{yi,x} \\ H_{i,y} & H_{xi,y} & H_{yi,y} & H_{xi,y} & H_{\gamma i,y} \\ R_{i,y} + H_{i,x} & R_{xi,y} + H_{xi,x} & R_{yi,y} + H_{yi,x} & R_{\gamma i,y} + H_{xi,x} & R_{yi,y} + H_{\gamma i,x} \end{bmatrix} \quad (24)$$

where $(\)_{,x}$ denotes a differentiation with respect to x , $R_{\gamma i} = R_{xi} - L_i$ and $H_{\gamma i} = H_{yi} - L_i$.

$$\mathbf{B}_s = [\mathbf{B}_{s1} \quad \mathbf{B}_{s2} \quad \mathbf{B}_{s3}] \quad (25)$$

$$\mathbf{B}_{si} = \begin{bmatrix} 0 & 0 & 0 & L_i & 0 \\ 0 & 0 & 0 & 0 & L_i \end{bmatrix} \quad (26)$$

3.1 Comments on element DST-S6

(1) It is clear that if the transverse shear effects are not important (for thin plates) the DST-S6 will convergence to the DKT. The DST-S6 is completely locking free and passes all constant patch tests exactly.

(2) It is clear from the above procedures that the formulation and the numerical implementation of the present stiffness matrices of the DST-S6 are much simpler than

that of the existing shear-deformable triangular plate elements currently available, which also pass the patch test for thin and thick plates.

(3) The DST-S6 has five DOF per node, which increases the computational cost of the final set of algebraic equations in the present method. However, the computational cost for generating the element stiffness matrix of the DST-S6 is much less than that of the other shear-deformable triangular plate elements, e.g., the DST-BL and DST-BK. In practical applications, the DST-S6 is more favorable than the other shear-deformable plate elements since it leads to a much simpler explicit expression and more efficient evaluation of the stiffness matrix.

(4) The DST-S6 has five DOF per node, but the two extra shear DOF (γ_{xi} and γ_{yi}) are actually rotations causing by the transverse shear deformation, as shown in Fig.3, and thus there is no difficulty to apply the essential boundary condition for the present DST-S6. For example, for the symmetric boundary shown in Fig.4, the boundary conditions of DST-S6 can be imposed in a weaker sense as follows

$$\begin{aligned} x = 0 : \quad & \theta_{xi} = 0, \quad \gamma_{xi} = 0 \\ y = 0 : \quad & \theta_{yi} = 0, \quad \gamma_{yi} = 0 \end{aligned} \tag{27}$$

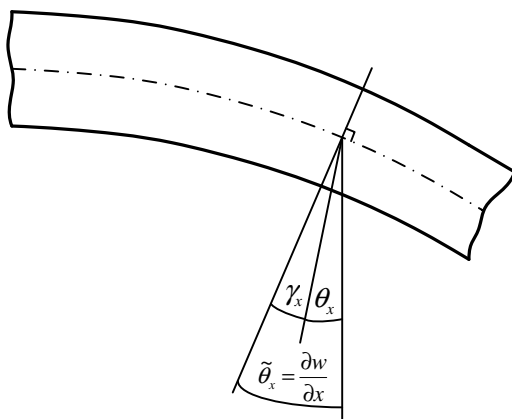


Figure 3: The transverse shear strain

4 Numerical examples

In this section, several problems have been solved to demonstrate the performance of the present DST-S6. The T3, DST-BL and RDKTM elements have been selected for comparison with the proposed DST-S6, where

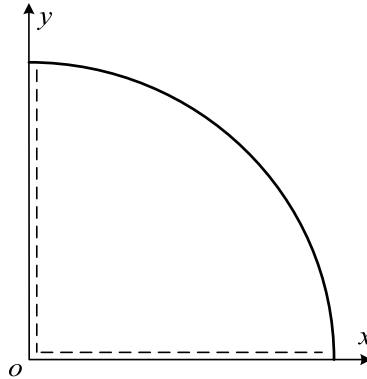


Figure 4: Symmetric boundary condition

T3: The triangular displacement element with full integration.

DST-BL: Discrete Mindlin triangular plate element proposed by Baotz and Lardeur(1989).

RDKTM: Re-constituting discrete Kirchhoff triangular plate element by Chen and Cheung (2001).

4.1 Eigenvalues and rank

Only three eigenvalues corresponding to the three rigid body modes (not including the shear DOF γ_{xi} and γ_{yi}) are always zero for various element shapes and for very thin to thick plates. The element has always a proper rank.

4.2 Constant curvature patch tests

The element stiffness matrix must satisfy the patch test in order to give reliable results. To check the performance of the element, we start with the patch test suggested in Batoz and Katili (1992), and Katili (1993).

We consider a patch of four elements as shown in Fig.5. The assumed material properties of the plate are $E = 1000$ and $\nu = 0.3$. The thickness of the plate is h . The characteristic length of the plate is l . The patch tests are performed by enforcing the following boundary conditions which lead to constant curvatures and zero transverse shear

Case A: $w = x^2/2; \theta_x = x; \theta_y = 0; \gamma_x = 0; \gamma_y = 0$

Case B: $w = y^2/2; \theta_x = 0; \theta_y = y; \gamma_x = 0; \gamma_y = 0$

Case C: $w = xy/2; \theta_x = y/2; \theta_y = x/2; \gamma_x = 0; \gamma_y = 0$

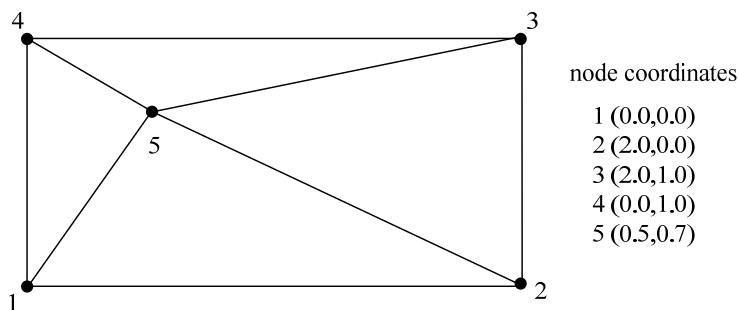


Figure 5: Mesh for the patch test

For the element DST-S6 exact results are obtained for any aspect ratio. But for the element DST-BL small errors appear for $h/l > 0.1$. The errors on the displacement w at node 5 are reported on Fig.6.

4.3 Constant shear patch tests

For verification of the constant shear deformation condition and zero curvature of the DST-BL and DST-S6, the following fields have been imposed on the boundary nodes in Fig.5:

Case A: $w = x/2$; $\theta_x = -1/2$; $\theta_y = 0$; $\gamma_x = 1$; $\gamma_y = 0$

Case B: $w = y/2$; $\theta_x = 0$; $\theta_y = -1/2$; $\gamma_x = 0$; $\gamma_y = 1$

Fig.7 shows the displacement w of node 5 for different thickness/length ration. It can be seen that the displacements approached the pure shear line at high values of h/l , and thus the elements DST-BL and DST-S6 pass the constant shear patch tests.

4.4 Square plate under uniform load

A simply supported or clamped square plate under uniform load q is considered for linear elastic analysis. The side length and the thickness of the square plate are l and h . A quarter of the plate is modeled due to the symmetry as shown in Fig.8.

The results for the central displacement w_0 and for the central bending moment M_0 for the simply supported plate are listed reported in Tabs.1 and 2. The results for the central displacement w_0 for the clamped plate are reported in Tab.3. As can be seen, the displacement solutions of the DST-S6 based on primal methods converge from "BELOW", and overall good results are obtained for the new locking-free element DST-S6 compared to T3, DST-BL and RDKTM.

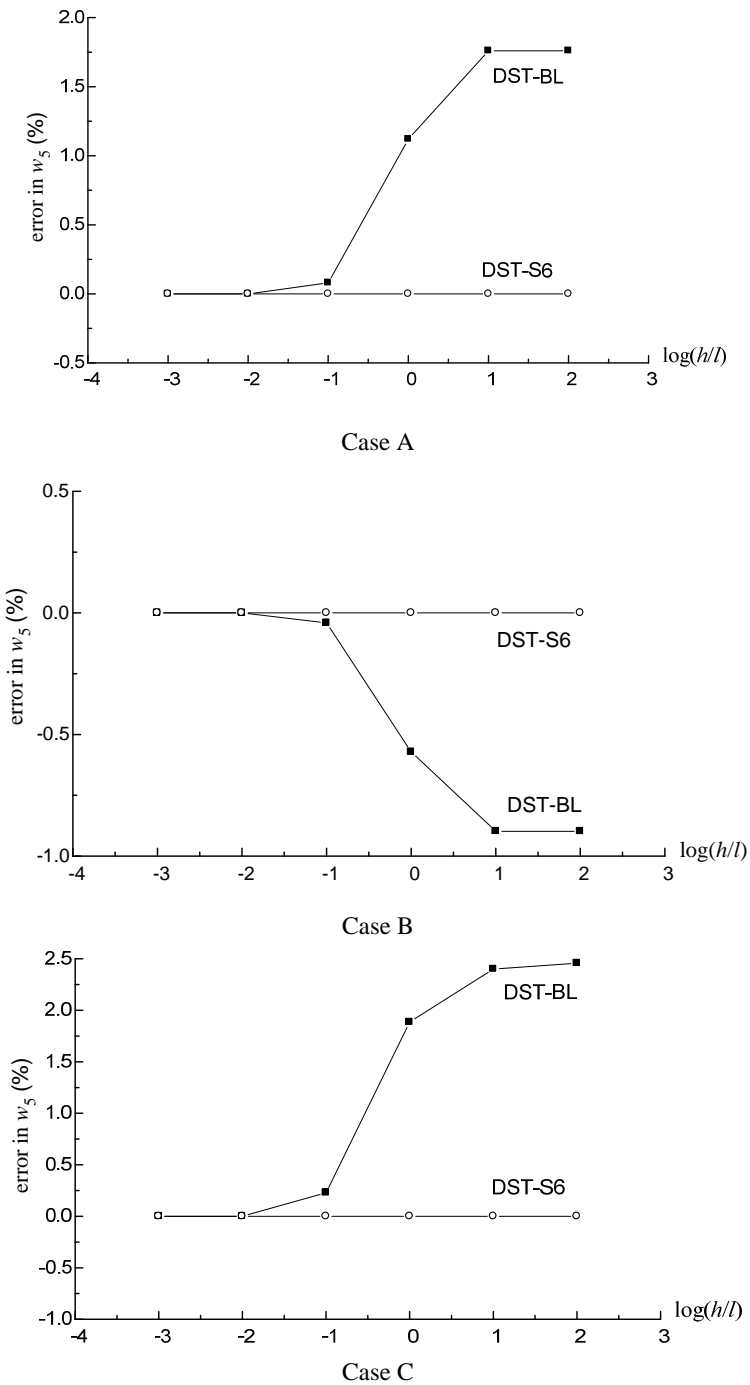


Figure 6: Constant curvature patch tests

Table 1: Central deflection ($\times ql^4/100D$) for a simply supported square plate loaded by uniform load

h/l	1.0e-5	0.001	0.01	0.10	0.15	0.20
DST-S6(2×2)	0.3681	0.3681	0.3684	0.3998	0.4333	0.4751
DST-S6(4×4)	0.3973	0.3973	0.3976	0.4230	0.4489	0.4834
DST-S6(8×8)	0.4040	0.4041	0.4044	0.4259	0.4505	0.4846
DST-S6(16×16)	0.4057	0.4057	0.4060	0.4260	0.4505	0.4848
DST-BL(16×16)	0.4057	0.4057	0.4059	0.4254	0.4498	0.4840
RDKTM(16×16)	0.4057	0.4057	0.4059	0.4256	0.4501	0.4844
T3(16×16)	—	—	0.0616	0.3999	0.4367	0.4755
Exact	0.4062	0.4062	0.4064	0.4273	0.4536	0.4906

Table 2: Central moment ($\times ql^2/10$) for a simply supported square plate loaded by uniform load

h/l	1.0e-5	0.001	0.01	0.10	0.15	0.20
DST-S6(2×2)	0.4637	0.4637	0.4638	0.3998	0.4874	0.4963
DST-S6(4×4)	0.4633	0.4633	0.4634	0.4689	0.4707	0.4717
DST-S6(8×8)	0.4614	0.4614	0.4615	0.4637	0.4640	0.4641
DST-S6(16×16)	0.4607	0.4607	0.4608	0.4614	0.4615	0.4615
DST-BL(16×16)	0.4607	0.4607	0.4604	0.4589	0.4585	0.4584
RDKTM(16×16)	0.4607	0.4607	0.4606	0.4605	0.4606	0.4606
T3(16×16)	—	—	—	0.4186	0.4402	0.4482
Exact	0.4789					

Table 3: Central deflection ($\times ql^4/100D$) for a clamped square plate loaded by uniform load

h/l	1.0e-5	0.001	0.01	0.10	0.15	0.20
DST-S6(2×2)	0.1212	0.1212	0.1214	0.1341	0.1498	0.1710
DST-S6(4×4)	0.1257	0.1257	0.1259	0.1428	0.1634	0.1914
DST-S6(8×8)	0.1263	0.1263	0.1266	0.1463	0.1702	0.2025
DST-S6(16×16)	0.1265	0.1265	0.1267	0.1478	0.1730	0.2073
DST-BL(16×16)	0.1265	0.1265	0.1267	0.1473	0.1723	0.2069
RDKTM(16×16)	0.1265	0.1265	0.1267	0.1486	0.1750	0.2108
T3(16×16)	—	—	0.0277	0.1425	0.1714	0.2081
Exact	0.1265	0.1265	0.1265	0.1499	0.1798	0.2167

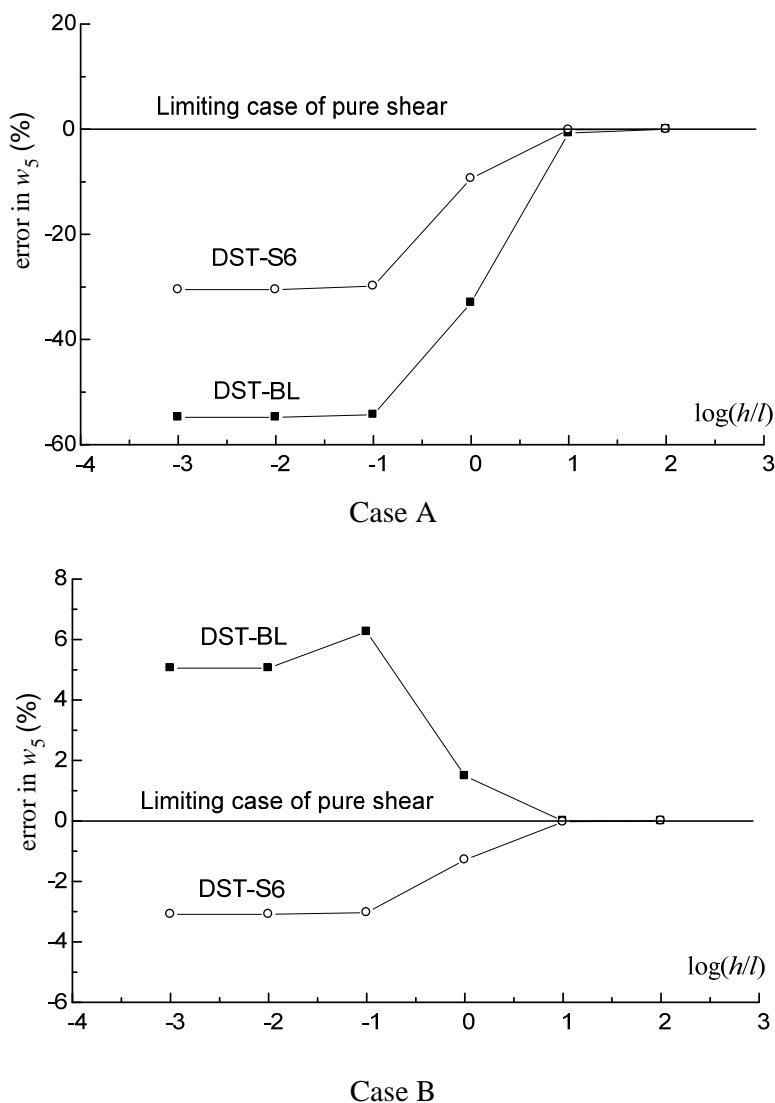


Figure 7: Constant shear patch tests

4.5 Clamped circular plate under uniform load

A clamped circular plate subjected to uniformly distributed load q is considered. The radius of the plate is $r = 100$ and the thickness of the plate is h . The material properties are $E = 100$ and $\nu = 0.3$. Due to the double symmetry, only one quarter

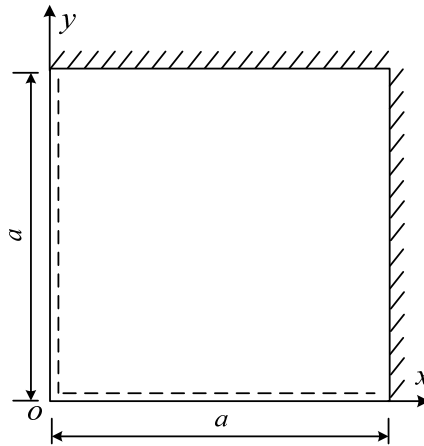


Figure 8: Model of a clamped square plate

of the plate is discretized as shown in Fig. 9. Four distributions of 25, 81 and 289 nodes are employed for the convergence studies. Similar good results are obtained by the present element DST-S6, as listed in Tab. 4. Numerical results also indicate that, although the primal methods are used, the displacement solutions of the example converge from "UP" for the DST-S6, DST-BL and RDKTM (except for the element T3).

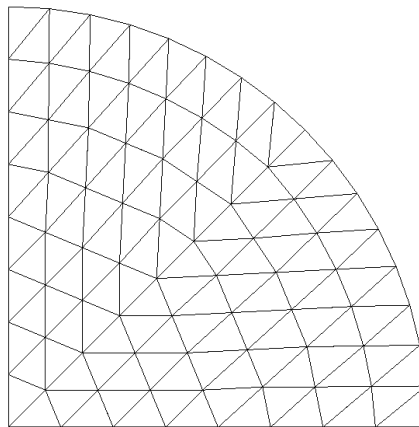


Figure 9: Mesh of one quarter of a clamped circular plate (81 nodes)

Table 4: Central deflection ($\times qr^4/100D$) for a clamped circular plate loaded by uniform load

h/r	1.0e-5	0.001	0.01	0.10	0.15	0.20
DST-S6(25)	1.6126	1.6126	1.6133	1.6759	1.7550	1.8656
DST-S6(81)	1.5758	1.5758	1.5765	1.6425	1.7259	1.8426
DST-S6(289)	1.5659	1.5659	1.5666	1.6348	1.7209	1.8415
DST-BL(289)	1.5659	1.5659	1.5666	1.6458	1.7395	1.8678
RDKTM(289)	1.5659	1.5659	1.5666	1.6368	1.7261	1.8513
T3(289)	—	—	0.1609	1.5009	1.6600	1.8112
Exact	1.5625	1.5625	1.5632	1.6339	1.7232	1.8482

4.6 Simply supported circular plate under uniform load

A simply supported circular plate subjected to uniformly distributed load q is considered. The geometry and the material properties of the plate are the same as the clamped circular plate. The method proposed by Rhee and Atluri (1986) is employed to impose the geometrical boundary conditions for the simply supported circular plate when a polygonal domain approximation is used. Tab. 5 demonstrates that the solution of the present DST-S6 avoids the so-called Babuska Paradox, by imposing the correct boundary condition. Numerical results also indicate that the displacement solutions of the DST-S6 based on primal methods converge from "BELOW", and overall good results are obtained for the new locking-free element DST-S6 compared to T3, DST-BL and RDKTM.

Table 5: Central deflection ($\times qr^4/100D$) for a simply supported circular plate loaded by uniform load

h/r	1.0e-5	0.001	0.01	0.10	0.15	0.20
DST-S6(25)	6.3014	6.3014	6.3021	6.3734	6.4634	6.5894
DST-S6(81)	6.3535	6.3535	6.3542	6.4252	6.5148	6.6402
DST-S6(289)	6.3661	6.3661	6.3668	6.4376	6.5270	6.6521
DST-BL(289)	6.3661	6.3661	6.3668	6.4505	6.5468	6.6773
RDKTM(289)	6.3661	6.3661	6.3667	6.4369	6.5263	6.6514
T3(289)	—	—	1.3514	6.2084	6.4245	6.5953
Exact	6.3702	6.3702	6.3709	6.4416	6.5309	6.6559

5 Conclusions

A new locking-free triangular plate element DST-S6 having three nodes, and five DOF per node, has been proposed. The two extra transverse shear strains (γ_{xi} and γ_{yi}) are introduced as additional shear DOF to eliminate the shear locking phenomenon for shear-deformable plates, but the extra shear DOF of the DST-S6 can be treated as rotations caused by the transverse shear deformation, and there is no difficulty to impose the essential boundary condition for the present DST-S6. The most promising feature of the DST-S6 is the simplicity of its formulation and its numerical implementation. Numerical examples indicate that the proposed DST-S6 passes the curvature patch tests and the shear patch tests exactly, and has high convergence rates and high accuracy.

A whole family of shear-deformable triangular and quadrilateral plate elements can in fact be derived with the similar formulation of the DST-S6. The present element can be applied to the linear/nonlinear analysis of composite plates and shells as well.

Acknowledgement: The authors gratefully acknowledge the support of National Basic Research Program of China (973 Program: 2011CB013800), Program for Changjiang Scholars and Innovative Research Team in University(PCSIRT, IRT1029), and Kwang-Hua Fund for College of Civil Engineering, Tongji University. This research was also supported in part by an agreement of UCI with ARL/ARO with D.Le and A.Ghoshal as cognizant collaborators, and by the World Class University (WCU) program through the National Research Foundation of Korea funded by the Ministry of Education, Science and Technology (Grant no.: R33-10049).

References

- Atluri, S.N. (2005):** Methods of Computer Modeling in Engineering & Science. Tech Science Press.
- Batoz, J.L.; Bathe, K.J.; Ho, L.W.(1980):** A study of three-node triangular plate bending elements. *International Journal for Numerical Methods in Engineering*, Vol.15, pp.1771-1812.
- Bathe, K.J.; Dvorkin, E.N.(1985):** A four-node plate bending element based on Mindlin/Reissner plate theory and a mixed interpolation. *International Journal for Numerical Methods in Engineering*, Vol.21, pp.367–383.
- Batoz, J.L.; Katili, I.(1992):** On a simple triangular Reissner/Mindlin plate element based on incompatible modes and discrete constraints. *International Journal*

for Numerical Methods in Engineering, Vol.35, pp.1603–1632.

Batoz, J.L.; Lardeur, P.(1989): A discrete shear triangular nine d.o.f. element for the analysis of thick to very thin plates. *International Journal for Numerical Methods in Engineering*, Vol.29, pp.533–560.

Brasile, S.(2008): An isostatic assumed stress triangular element for the Reissner–Mindlin plate-bending problem. *International Journal for Numerical Methods in Engineering*, Vol.74, pp.971–995.

Cai, Y.C.; Paik, J.K.; Atluri S.N. (2009a): Large Deformation Analyses of Space-Frame Structures, with Members of arbitrary Cross-Section, Using Explicit Tangent Stiffness Matrices, Based on a von Karman Type Nonlinear Theory in Rotated Reference Frames. *CMES: Computer Modeling in Engineering & Sciences*, Vol. 53, No. 2, pp. 123-152.

Cai, Y.C.; Paik, J.K.; Atluri S.N. (2009b): Large Deformation Analyses of Space-Frame Structures, Using Explicit Tangent Stiffness Matrices, Based on the Reissner variational principle and a von Karman Type Nonlinear Theory in Rotated Reference Frames. *CMES: Computer Modeling in Engineering & Sciences*, Vol. 54, No. 3, pp. 335-368.

Cai, Y.C.; Paik, J.K.; Atluri S.N. (2010a): Locking-free Thick-Thin Rod/Beam Element for Large Deformation Analyses of Space-Frame Structures, Based on the Reissner Variational Principle and A Von Karman Type Nonlinear Theory. *CMES: Computer Modeling in Engineering & Sciences*, Vol. 58, No. 1, pp. 75-108.

Cai, Y.C.; Paik, J.K.; Atluri S.N. (2010b): A triangular plate element with drilling degrees of freedom, for large rotation analyses of built-up plate/shell structures, based on the Reissner variational principle and the von Karman nonlinear theory in the co-rotational reference frame. *CMES: Computer Modeling in Engineering & Sciences*, Vol. 61, pp.273-312.

Chen, W.J. and Cheung, Y. K.(2001): Refined 9-Dof triangular Mindlin plate elements. *International Journal for Numerical Methods in Engineering*, Vol.51, pp.1259–1281.

Choo, Y. S.; Choi, N.; Lee, B.C.(2010): A new hybrid-Trefftz triangular and quadrilateral plate elements. *Applied Mathematical Modelling*, Vol.34, pp.14–23.

Dhatt, G.(1969): Numerical analysis of thin shells by curved triangular elements based on discrete Kirchhoff hypothesis. Proc. ASCE Symp. on Applications of FEM in Civil Engineering, Vanderbilt University, Nashville, Tenn., pp. 255-278.

Gal, E.; Levy, R.(2006): Geometrically nonlinear analysis of shell structures using a flat triangular shell finite element. *Arch. Comput. Meth. Engng.*, Vol. 13, pp. 331-388.

Hughes, T.J.R.; Cohen, M.; Haroun, M.(1978): Reduced and selective integration techniques in finite element analysis of plates. *Nuclear Engineering and Design*, Vol.46, pp.203–222.

Iura, M.; Atluri, S.N.(2003): Advances in finite rotations in structural mechanics. *CMES: Computer Modeling in Engineering & Sciences*, Vol.4, pp.213-215.

Katili, I. (1993): A new discrete Kirchhoff-Mindlin element based on Mindlin-Reissner plate theory and assumed shear strain fields—part I: an extended DKT element for thick-plate bending analysis. *International Journal for Numerical Methods in Engineering*, Vol.36, pp.1859–1883.

Lee, S.W.; Pian, T.H.H.(1978): Improvement of plate and shell finite elements by mixed formulation. *AIAA Journal*, Vol.16, pp.29–34.

Li, Q.; Soric, J.; Jarak, T.; Atluri, S.N. (2005): A locking-free meshless local Petrov–Galerkin formulation for thick and thin plates. *Journal of Computational Physics*. Vol. 208, pp.116–133.

Malkus, D.S.; Hughes, T.J.R.(1978): Mixed finite element methods-reduced and selective integration techniques: a unification of concepts. *Computer Methods in Applied Mechanics and Engineering*, Vol.15, pp.63–81.

Nguyen, X.H.; Rabczuk, T.; Stephane, B.; Debongnie, J.F.(2008): A smoothed finite element method for plate analysis. *Computer Methods in Applied Mechanics and Engineering*, Vol.197, pp.1184–1203.

Pugh, E.D.; Hinton, E., Zienkiewicz, O.C.(1978): A study of triangular plate bending element with reduced integration. *International Journal for Numerical Methods in Engineering*, Vol. 12, pp.1059 –1078.

Rhee, H.C.; Atluri, S.N. (1986): Polygon-circle paradox in the finite element analysis of bending of a simply supported plate. *Computers & Structures*, Vol.22, pp.553-558.

Zhu, H.H.; Cai, Y.C.; Paik, J.K.; Atluri S.N. (2010): Locking-free Thick-Thin Rod/Beam Element Based on a von Karman Type Nonlinear Theory in Rotated Reference Frames For Large Deformation Analyses of Space-Frame Structures. *CMES: Computer Modeling in Engineering & Sciences*, Vol. 57, No. 2, pp. 175-204.

Zienkiewicz, O.C.; Taylor, R.L.; Too, J.M. (1971): Reduced integration technique in general analysis of plates and shells. *International Journal for Numerical Methods in Engineering*, Vol. 3, pp.275–290.